

A Hybrid Optimization Tool for Active Magnetic Regenerator

Author 1
University
City, Country
author@mail.com

Author 2
University
City, Country
author@mail.com

Author 3
University
City, Country
author@mail.com

Author 4
University
City, Country
author@mail.com

Author 5
University
City, Country
author@mail.com

Author 6
University
City, Country
author@mail.com

ABSTRACT

Active Magnetic Regenerator (AMR) refrigeration based on a temperature changing in Magneto Caloric Materials (MCMs) is an innovate technology, which can reduce energy consumption and the depletion of the ozone layer. However, to develop a commercially applicable design of the AMR model is still an issue, because of the difficulty to reproduce physical properties of different MCMs and to find a configuration of the AMR parameters, which are suitable for various applications needs. In this work, we focus on the optimization of a simulation model of AMR in two application modes: a magnetic refrigeration system and a thermo-magnetic generator. From an optimization point of view, the AMR problems are typical examples of black-box problems with different number of objectives. This paper proposes a robust optimisation tool based on a hybridisation of the Non-dominated Sorting Genetic Algorithm III and Quantum Particle Swarm Optimisation algorithm, which ensures the scalability with respect to the number of objectives and allows to easily set up optimisation experiments for different research cases. A thorough tool validation is presented. It is expected that this tool can help to make a qualitative jump in the development of AMR refrigeration.

CCS CONCEPTS

• **Computing methodologies** → **Artificial intelligence**; Modeling and simulation.

KEYWORDS

real-world application, hybridization, unified optimization

ACM Reference Format:

Author 1, Author 2, Author 3, Author 4, Author 5, and Author 6. 2022. A Hybrid Optimization Tool for Active Magnetic Regenerator. In *Proceedings of the Genetic and Evolutionary Computation Conference 2022 (GECCO '22)*. ACM, New York, NY, USA, 9 pages.

Permission to make digital or hard copies of all or part of this work for personal or classroom use is granted without fee provided that copies are not made or distributed for profit or commercial advantage and that copies bear this notice and the full citation on the first page. Copyrights for components of this work owned by others than ACM must be honored. Abstracting with credit is permitted. To copy otherwise, or republish, to post on servers or to redistribute to lists, requires prior specific permission and/or a fee. Request permissions from permissions@acm.org.

GECCO '22, July 9–13, 2022, Boston, USA

© 2022 Association for Computing Machinery.

ACM ISBN 978-x-xxxx-xxxx-x/YY/MM.

1 INTRODUCTION

Nowadays, the demand for cooling is increasing, due to the climate change and universal problems: e.g., the current pandemic of Covid-19. Since vaccines are roll out, they need enormous cold-storage systems for their manufacture, distribution and storage. According to a report by the *International Energy Agency*, the number of global cooling devices is estimated to increase from 3.6 billion to 9.5 billion by 2050.

In this context, in order to reduce worldwide electricity consumption and direct greenhouse gas emissions, Active Magnetic Regenerator (AMR) refrigeration is a promising technology, which replaces the cycles of gas compression/expansion by the phases of magnetization/demagnetization of solid refrigerants - Magneto Caloric Materials (MCMs) [1], [3]. An AMR consists of a porous matrix of MCMs, which is traversed by a fluid flow and is synchronized with a magnetic field variation. Its working principle is based on the reversible temperature change in MCMs, which occurs near the Curie temperature under applying magnetic field for producing cooling effect [11].

The AMR is a complex system, where multiple physical phenomena coexist and define its performance. Generally, to simplify a process of its development, a simulation model of the AMR is used, which comprises a model of MCMs for reproducing physical properties of several MCMs in order to provide the refrigeration over a temperature span comparable to conventional refrigeration.

Despite the promising researches, the AMR development has two principle problems that prevent its commercial production: (i) to simulate physical properties of different MCMs in good qualitative agreement with the available experimental data; (ii) to comprehensively tune many control and design parameters of the AMR model, depending on their effect on its performance.

For overcoming these difficulties, related researches apply optimization algorithms to the numerical simulation models of MCMs [13] and AMR [25], [7], [21]. However, the optimization has never been applied to the both problems in the frame of the same research study. Moreover, the common point of the works aiming at optimizing the AMR performance is to focus on only a single problem definition for a selected application mode. Thus, they do not allow to explore innovative architectures of AMR, which can operate in different application modes.

These restrictions are explained by the difficulty to set up new optimization experiments, where different number of objectives and decision variables are required. From an optimization point of view:

- the problems of the AMR design are the black-box optimization problems, where the number of decision variables is changing according to the number of control and design parameters and the number of objectives depends on the performance metrics taken into consideration;
- the problems of reproducing physical properties of MCMs are separable or partially seaprable optimization problems, where the number of objectives depends on the number of studied physical properties of materials.

If an optimization problem is modified so that its number of objectives is changed, to conduct a new experiment is a complicated and time-consuming task, because an efficient algorithm for finding the global optimum of a single-objective problem, cannot be adequately applied to find many optimal solutions for another optimization problem [5]. In this case, a user has to know different algorithms specialized in solving a particular number of objectives. Moreover, every time when the problem is reformulated/changed, a user must merge the codes of this new problem and a new algorithm. Thus, the scientific and practical necessity in a robust algorithm scalable w.r.t. the number of objectives (and decision variables) is obvious.

For improving optimization process of the AMR design, we present an user-friendly optimization tool based on an “unified” algorithm. The term “unified” is borrowed from [22], where it was introduced for describing the algorithms, which ensure the scalability w.r.t. the number of objectives: i.e., capable to solve from single- to many-objective problems. In the presented unified algorithm, we extend the idea proposed in [22], to scale the well-known many-objective Non-dominated Sorting Genetic Algorithm III (NSGA-III) down to solve single-objective problems. But comparatively with [22], we employ a hybridization for fusing the solutions of NSGA-III with the solutions of Quantum Particle Swarm Optimization (QPSO) algorithm, instead of the modifications of NSGA-III structure. This hybridization allows NSGA-III to handle very small population size in single-objective cases, which is useful for optimizing computationally intensive problems. To our best knowledge, this work is the first attempt to apply hybridization to unified optimization.

Applying presented optimization tool, we show in this work that:

- the proposed unified algorithm is robust for solving a single-objective problem in order to reproduce physical properties of MCMs;
- it is possible to find the common configuration of control and design parameters for the AMR, which is operating in two modes: Magnetic Refrigeration System (MRS) and Thermo-Magnetic Generator (TMG). To our best knowledge, there are no researches, which simultaneously optimize the design of the AMR model for two operating modes.

Compiling all together, we want to contribute by making a step forward the further development of AMR refrigeration for its commercial application and a new insight about hybrid method, which is capable to be employed for constituting scalable algorithms.

This paper is organized as follows. Section 2 describes the materials and methods. The experiments and results are shown in Section 3. Finally, Section 4 presents some conclusions.

2 MATERIALS AND METHODS

2.1 The Simulation Models

The simulators used for this project are presented in the two following subsections.

2.1.1 The model of Magneto Caloric Materials. In this work, we use a method for studying/reproducing physical properties of MCMs presented in [13]. It is based on the generalize Blume-Emery-Griffiths-Ising (BIG-I) Hamiltonian model of MCMs, which is provided by the Crismat laboratory¹ and briefly described in [13]. From an optimization point of view, the proposed method can be considered as:

- (1) a computationally intensive problem: the average execution time of one run of a Monte Carlo solver of the BEG-I model is 4h on AMD EPYC 7371 16-Core Processor;
- (2) a continuous optimization problem;
- (3) a separable/partially separable problem, because its Hamiltonian presents the sum of three parts, where each of these part is calculated with one or two independent decision variables;
- (4) from single- to multi-objective problems.

2.1.2 The model of Active Magnetic Regenerator. The AMR model is provided by Ubiblu Company and is under active development since 2013. The AMR model takes into account the five following components: the regenerator (the matrix of MCMs), the hot and cold heat exchangers, the pump and the magnet. Thus, this model is a multi-physic and multi-scale model, where: (i) a magnetic model is represented at micro scale by the electron’s spins alignment under an applied magnetic field; (ii) a fluid flow is represented at mini scale by the heat transfer fluid and (iii) a heat transfer is represented at macro scale by the thermal exchange via the heat transfer fluid [19]. Figure 1 presents a basic scheme of this magnetic device [19]. More details about the AMR model can be found in the publicly available description in [19] and in [15]. In this work, we deal with extended version of the AMR model, which can operate in two modes: as the Magnetic Refrigeration System (MRS) and the Thermo-Magnetic energy Generator (TMG).

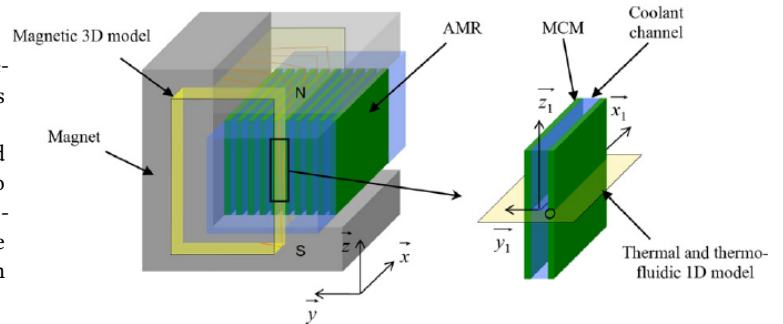


Figure 1: The basic scheme of a magneto caloric device. The illustration is adapted from [19].

Table 1 reports the common AMR configuration for the MRS and the TMG modes, which is used for all simulations in this

¹<https://crismat.cnrs.fr/>

Table 1: Default parameters of AMR model configuration for both operating modes

Parameter	Value	Unit
Geometry type	parallel plates	[-]
MCMs data set	<i>FeSiLaMnH</i> -based	[-]
Plate thickness	0.4	[mm]
Fluid channel thickness	0.15	[mm]
Magnetic field change value	0 - 0.8	[T]
Temperature span	0 - 65	[°C]
T_c segment layering length	1	[cm]

work. These configuration parameters were chosen according to the feedback from previous Ubibblue prototypes and corresponds to a technical-economical optimum.

From an optimization point of view, the AMR model of Ubibblue is considered as:

- (1) a computationally intensive problem: the execution time of one simulation run of a single-mode operating AMR model has high variance and takes 15h max. on AMD EPYC 7371 16-Core Processor;
- (2) a continuous optimization problem;
- (3) a black-box optimization problem;
- (4) a small, medium and large scale problem, where the number of decision variables depends on the number control and design parameters, which are taken under consideration;
- (5) from single- to many-objective problems.

2.2 Hybrid Unified Optimization Algorithm

Aiming at ensuring the scalability w.r.t. the number of objectives for time-consuming problems, we develop further the idea of unified algorithm presented in [22], by employing a hybridization method for scaling down a many-objective algorithm to single-objective optimization.

Non-dominated Sorting Genetic Algorithm III (NSGA-III) originally presented in [4], is selected as a baseline many-objective algorithm in this work, because of the following reasons: (i) it has a small number of turning parameters; (ii) it has an ability to efficiently solve different many-objective problems and (iii) it was already used for the unified optimization in [22].

However, as it was explained in [22], NSGA-III can not efficiently solve single-objective problems, because of the following features of NSGA-III:

- (1) The recommended population size for single objective optimization equals 4 solutions (defined as the smallest multiple of 4 greater than the number of reference directions, where only one reference direction is considered in case of single objective optimization), which is too small for NSGA-III's recombination operator to find useful child solutions.
- (2) The solutions are picked randomly for recombination/mutation operators, which means that with growing population size, without selection pressure, NSGA-III will work as a random walk algorithm on single-objective problems. Consequently,

the algorithm will require larger number of calls of evaluation functions, which is an issue for computationally intensive problems.

Instead of increasing the population size and adding the selection pressure, as it was proposed in [22], we employ a hybridisation method by fusing the solutions from different algorithms. In general, a hybridisation method combines the solutions from two or more algorithms such that the resulting algorithm extracts the best solutions by exploiting the different features of all integrated algorithms for solving larger number of problems [26], [10].

For single-objective optimization, in order to maintain the diversity in the NSGA-III population with only 4 solutions, we propose to fuse the solutions of NSGA-III with the solutions of Quantum-inspired Particle Swarm Optimization algorithm (QPSO). For the sake of avoiding redundancy, we do not provide the description of the original NSGA-III and QPSO algorithms.

The QPSO algorithm presented in [24], uses the concept of quantum particle motion in the Delta potential well for reaching the optimal solution. QPSO is selected as an auxiliary algorithm in this hybrid method, because of the following reasons: (i) it is theoretically guaranteed that QPSO converges to the global optimum and (ii) QPSO has been successfully applied to a vast variety of engineering problems [6], [29], [12] and [14]. However, QPSO has several limitations:

- the minimal recommended population size is 20 solutions [24], which is a critical condition, since QPSO and NSGA-III have to work with the same population size of 4 solutions in the hybrid algorithm;
- an impact of the contraction expansion parameter (α) on the performance, which has to be somehow adjusted.

In order to overcome these limitations, we propose the modified version of QPSO presented in the following subsection.

2.2.1 The Modified QPSO Algorithm. In fact, the both presented above limitations of QPSO are connected with a lack of control of the population diversity. Indeed, according to the quantum physics, the width of the Delta potential well ($L_{i,j}$ in Algorithm 1) determines the search space of each particle at each generation. Its value goes to zero during the optimization process, where the ground state has to be found. This width is depends on the value α and the deference between the mean coordinates of the personal best positions of all particles and the coordinates of the current particle (see lines 15 in Algorithm 1). If the population has a small size, the value of $|p_{mean} - r|$ will be prematurely around zero, and consequently, the width of the Delta potential well will be prematurely too narrow.

Is is supposed that the parameter α can help to improve this issue, which aims at controlling the convergence behaviour and the diversity adjustment. However, a method to select the value of α is still opened topic and studied in more recent researches: [23], [17], [18] and [27]. However, all of these methods depend on the total number of generations and no one of them can work efficiently with the small population size. In such cases, the total number of generations becomes very important tuning parameter, which determines the performance.

Instead of adjusting the parameter α according to the total number of generations, we propose to integrate the coefficient of control

Table 2: Notations used in Algorithm 1

Notation	Explication	Value
t	current generation	$t \in \mathbf{N}_+$
N	population size	$t \in \mathbf{N}_+$
d	number of coordinates	$d \in \mathbf{N}_+$
\mathbf{r}^t	particle position	$\mathbf{r}^t \in \mathbb{R}^d$
i	index of current particle	$i \in \mathbf{N}_+$
j	index of current coordinate	$j \in \mathbf{N}_+$
c_p, c_g	random numbers uniformly distributed	$c_p, c_g \in \mathbb{R}$
$\mathbf{p}_i^{(t)}$	the local attractor for i -th particle	$\mathbf{p}_i^{(t)} \in \mathbb{R}^d$
$\mathbf{p}_{mean}^{(t)}$	mean value of local best position	$\mathbf{p}_{mean}^{(t)} \in \mathbb{R}^d$
$\mathbf{r}_{best(i)}^{(t)}$	the best local position of i -th particle	$\mathbf{r}_{best(i)}^{(t)} \in \mathbb{R}^d$
$\mathbf{r}_{best(g)}^{(t)}$	the best global position	$\mathbf{r}_{best(g)}^{(t)} \in \mathbb{R}^d$
$L_{i,j}^{(t)}$	width of Delta potential well	$L_{i,j}^{(t)} \in \mathbb{R}$
c_{div}	diversity coefficient	$c_{div} \in \mathbb{R}$
c_{limit}	boundary value of c_{div}	$c_{limit} \in \mathbb{R}$
α	contraction-expansion coefficient	$\alpha \in \mathbb{R}_+$
\mathcal{C}	Cauchy distribution	
\mathcal{U}	Uniform distribution	

of the diversity and to directly change the width of the potential well, without extra manipulations with value of α .

The pseudo-code of this modified procedure is given in Algorithm 1 and its notation is presented in Table 2. Comparatively to the original version of QPSO presented [24], the following modifications are integrated:

- (1) a static value of $\alpha = 0.75$ is used, which selected experimentally on different classes of problems;
- (2) a special coefficient c_{div} is integrated in order to control the diversity:

$$c_{div}^{(t)} = \frac{1}{N} \sum_{i=1}^N \sum_{j=1}^d |r_{i(j)}^{(t)} - p_{mean(j)}^{(t)}| \quad (1)$$

where $r_{i(j)}^{(t)}$ is a j -th coordinate of i -th particle; $p_{mean(j)}^{(t)}$ is a j -th coordinate of the mean value of the personal best positions of all particles; N is the population size; d is the dimension of search space; t is the current generation.

- (3) if the value of c_{div} is smaller than the threshold value $c_{limit} = 0.0001$, a small Cauchy distributed random noise is introduced in each coordinate of particle: the value of c_{div} replaces $L_i^{(t)}$ (line 13 in Algorithm 1). The heavy tails of Cauchy distribution is selected, since they are more efficient comparatively with the exponentially decreasing tails of Gaussian distribution, because the long jumps can lead to better solutions [28], [9]. Moreover, uni-variant Cauchy distribution is heavily coordinate-dependent and consequently, can be efficient on separable functions, which is useful for solving the separable problems of the model of MCMs.

Algorithm 1: The modified QPSO algorithm.

Result: returns the position vector of the global best particle

```

1 begin
2   Initialize the current positions randomly
3    $\alpha = 0.75$ 
4   for  $t = 1$  to  $T$  do
5      $\mathbf{p}_{mean}^{(t)} =$ 
6        $\left( \frac{1}{N} \sum_{i=1}^N \mathbf{r}_{best(i)}^{(t)}, \frac{1}{N} \sum_{i=1}^N \mathbf{r}_{best(2)}^{(t)}, \frac{1}{N} \sum_{i=1}^N \mathbf{r}_{best(d)}^{(t)} \right)$ 
7     Calculate  $c_{div}$  using Eq. 1
8     for  $i = 1$  to  $N$  do
9       Calculate fitness  $f(\mathbf{r}_i^{(t)})$ 
10       $\mathbf{r}_{best(i)}^{(t)} = \left\{ \begin{array}{l} \mathbf{r}_{best(i)}^{(t)}, \quad f(\mathbf{r}_i^{(t)}) \geq f(\mathbf{r}_{best(i)}^{(t)}) \\ \mathbf{r}_i^{(t)}, \quad f(\mathbf{r}_i^{(t)}) \leq f(\mathbf{r}_{best(i)}^{(t)}) \end{array} \right\}$ 
11       $\mathbf{r}_{best(g)}^{(t)} = \arg \min_{\mathbf{r}_{best(i)}^{(t)}} f(\mathbf{r}_{best(i)}^{(t)})$ 
12       $c_p, c_g \sim \mathcal{U}[0, 1]$ 
13      Compute local attractor:
14       $\mathbf{p}_i^{(t)} = \frac{c_p \cdot \mathbf{r}_{best(i)}^{(t)} + c_g \cdot \mathbf{r}_{best(g)}^{(t)}}{c_p + c_g}$ 
15      for  $j = 1$  to  $d$  do
16        if  $c_{div} < c_{limit}$  then
17           $L_{i,j} = \mathcal{C}(0, c_{div})$ 
18        else
19           $L_{i,j} = (2 \cdot \alpha) \cdot |p_{mean(i,j)}^{(t)} - r_{i,j}^{(t)}|$ 
20        if  $(\mathcal{U}[0, 1] < 0.5)$  then
21           $r_{i,j}^{(t+1)} = p_{i,j}^{(t)} - L_{i,j} \cdot \ln(1/u)$ 
22        else
23           $r_{i,j}^{(t+1)} = p_{i,j}^{(t)} + L_{i,j} \cdot \ln(1/u)$ 
24      return  $\mathbf{r}_{best(g)}$ 

```

2.2.2 The Hybrid Algorithm. The structure of the proposed hybrid algorithm, called QIU-NSA, is shown in Figure 2. The explanation of this structure is provided below. It consists of three main modules: NSGA-III, the modified QPSO and the fusion module. Note that multi- and many-objective problems are solved by NSGA-III, i.e., the proposed hybridisation is active only for single-objective problems.

At generation $t = 0$, the algorithm starts in the fusion module with the definition of the following parameters: (i) the dimension of search space (d); (ii) the dimension of objective space (m); (iii) the vectors of boundaries (\mathbf{lb} , \mathbf{ub}) for each decision variable; (iv) the threshold of diversity (c_{limit}) and (v) the total number of generations (T_{max}). The diversity coefficient (c_{div}) is set to 0. The termination criterion is defined as the total number of generations.

In the fusion module, the initial population $\mathbf{P}^{t=0}$ are created randomly according to the defined boundaries (\mathbf{lb} , \mathbf{ub}) and evaluated.

Then, the following steps are iterated until the termination criterion is satisfied:

- (1) **Make Child Population:** The parent population P^t is sent to NSGA-III and QPSO modules in order to produce the new child populations. Each module, NSGA-III and QPSO, creates new set of solutions $Q_{NSGA-III}^{t+1}$ and Q_{QPSO}^{t+1} according its original rules and returns them into the fusion module.
- (2) **Uniform-based Random Selection:** In the fusion module, the populations $Q_{NSGA-III}^{t+1}$ and Q_{QPSO}^{t+1} are used to select 4 solutions to the next population Q^{t+1} by the rule based on the Uniform distribution:
if uniformly distributed random number $\mathcal{U}(0, 1) > 0.5$, the solution of Q_{QPSO}^{t+1} is accepted, otherwise - $Q_{NSGA-III}^{t+1}$.
- (3) **Evaluation of Q^{t+1} :** The obtained population Q^{t+1} is evaluated and is sent back with their evaluated values to the QPSO and NSGA-III modules.
- (4) **Selection to the Next Generation:** The QPSO and NSGA-III modules have the same candidates for the next population P^{t+1} . Since NSGA-III is a core of the hybrid algorithm, the solutions for the next parent population P^{t+1} will be selected according to the procedure of NSGA-III. Independently, QPSO updates the local best solutions and defines the global solution among the local best solutions according to its original rules presented in [24]. At the end of the generation t , the QPSO module returns current global solution g^{t+1} and the NSGA-III module returns the new parent population P^{t+1} to the fusion module.

At the end of the optimization process, when $t = T_{max}$:

- in the case of single-objective optimization: the best solution is found in the current global solution g^{t+1} ;
- in the case of multi-/many-objective optimization: the optimal solutions are found in the optimal Pareto front provided by NSGA-III.

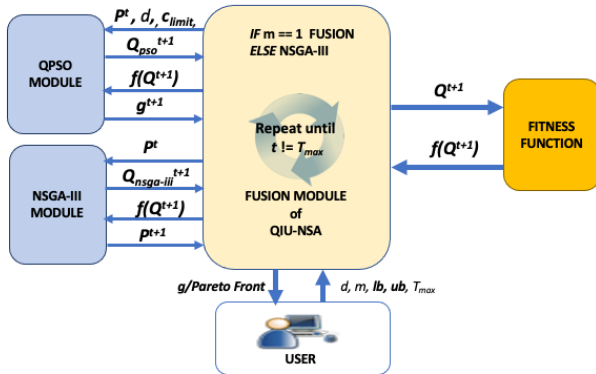


Figure 2: Simplified scheme of the unified algorithm.

Figure 3 shows how the integrated diversity coefficient of the QPSO algorithm helps to achieve the global optima of Rastrigin-Bueche function during the evaluation process.

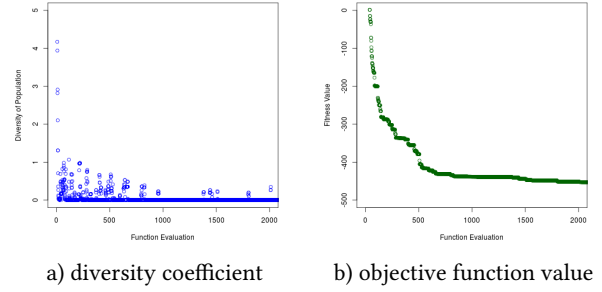


Figure 3: Diversity coefficient and objective function value w.r.t. the number of evaluations on Rastrigin-Bueche function

To summarise, the hybrid method allows to scale NSGA-III down to solve single-objective problems without any modifications in the NSGA-III structure, which excludes a risk to loss its effectiveness on multi-/many-objective problems. It does not need any additional parameters. We believe that the proposed algorithm not only allows to solve the different problems of the simulation models, but also presents an application of a quantum-inspired algorithm inside a hybrid method, which can be beneficial for further researches.

2.3 Optimization Software Tool

An user-friendly interface is required in order to simplify a code-coupling process between each research problem and the proposed unified algorithm. For this purpose, we extend the optimization tool presented in [13], which is based on the open-source EASEA (*EAsy Specification of Evolutionary Algorithms*) platform, by implementing QIU-NSA as a template of the EASEA platform. The EASEA provides a compiler for automatically merging a problem description file **.ez*, which specifies a scientific research task, with an optimization algorithm template into a CPU parallel C++ code [2]. It significantly simplifies to set up a new experiment and gives a large degree of freedom for scientists, because the codes of the problems and the simulation models can be modified independently from the optimization algorithm. Moreover, the models can be a source code on different programming languages or an executable file.

In order to specify the research problems, the following problem attributes have to be defined in the file **.ez*:

- (1) **Configuration:** (i) problem configuration - types of decision variables and objectives, dimension of search space and of target space, boundaries of each variable; (ii) algorithm configuration - types of crossover and mutation operators and their parameters; (iii) optional - reference values or needed constants.
- (2) **Evaluator:** (i) call the external model code; (ii) optional - call a post-processing unit, which transforms the output of the model to the input parameters of the objective functions; (iii) the objective function(s).

For further information, the detailed users' guide is provided in the EASEA online documentation ².

Once a problem description file is done, the presented tool can be run by doing the next three steps:

- (1) to compile the file, containing the problem specification, with the unified algorithm template into a CPU parallel C++ code;
- (2) to compile the obtained C++ code into an executable code;
- (3) to run the executable file with the desired number of parallel threads.

These optimization problems of reproducing physical properties of MCMs and the AMR model design are formulated as:

- (1) minimization of one/several differences between simulated and reference physical properties of MCMs for finding optimal parameters of the Hamiltonian of the BEG-I model;
- (2) maximization of efficiency and/or power density for the MRS and/or the TMG operating modes for finding optimal control and design parameters of the AMR model.

3 EXPERIMENTS AND RESULTS

The validation of the proposed optimization tool consists of the following experiments:

- Confirm an ability of the proposed hybrid unified algorithm, QIU-NSA, to solve single-objective problems on different dimensions of search space.
- Reproduce the physical properties of interest for *LaFeCoSi* alloy and to compare them *versus* the experimentally measured values, provided by the Crismat laboratory.
- Find the common configuration of control and design parameters of the AMR, for its application as the Magnetic Refrigeration System (MRS) and the Thermo-Magnetic Generator (TMG).

3.1 Validation of the Hybrid Unified Algorithm

We benchmark QIU-NSA on 24 functions of the Black-Box Optimization Benchmarking (BBOB) single-objective test suite and on its large-scale extension [8] provided by the COmparing Continuous Optimizers (COCO) platform³. The reported results are based on 15 independent run of 15 instances of each function. The Empirical Cumulative Distribution Functions (ECDF) presented in [8] and aggregated by the functions groups and by dimensions is used as a performance metrics. The parameter settings of the algorithms are presented in Table 3.

Table 3: Parameter settings of peer algorithms

Parameter	NSGA-III	QPSO	QIU-NSA
SBX p_c	1.0	-	1.0
SBX η_c	30	-	30
Poly. mut. p_m	$1/d$	-	$1/d$
Poly. mut. η_m	20	-	20
α	-	linearly decreasing	0.75

²<http://easea.unistra.fr>

³<https://github.com/numbbo/coco>

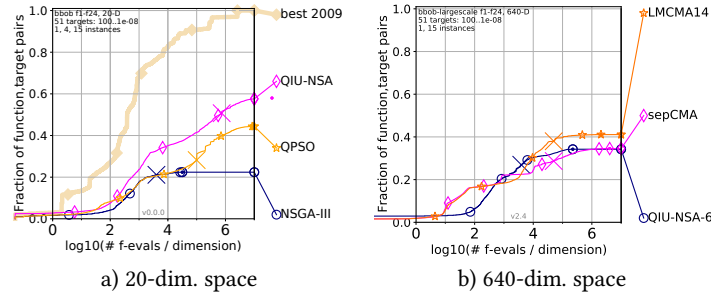


Figure 4: The ECDF summarized by function groups

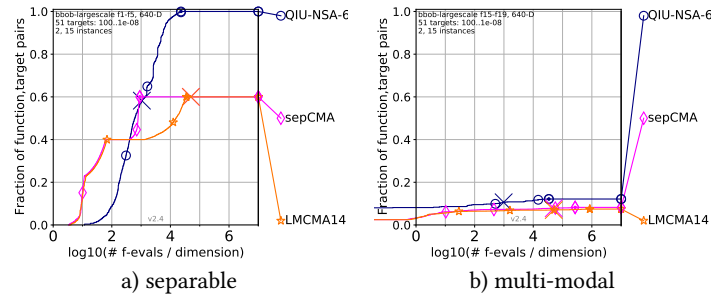


Figure 5: The ECDF summarized by separable and multi-modal functions on 640-dimensional search space

The comparative results of QIU-NSA *versus* the original NSGA-III and QPSO are presented in Figure 4 a), where each graph depicts the ECDF summarized by all 24 functions on 20-dimensional search space. As seen from Figure 4 a), QIU-NSA solves 60% of problem, followed by QPSO with 42% and NSGA-III with only 20% of solved functions. The obtained results confirm the workability of the proposed hybrid unified algorithm.

Taking into account that the AMR design problems can be large scale, we compare the performance of QIU-NSA on 640-dimensional search space with the reference results of separable CMA-ES (sepSMA) [20] and Limited Memory CMA-ES (LMCMA-ES) [16] provided by COCO platform. Looking at the aggregated ECDFs of all functions in Figure 4 b), we observe that QIU-NSA and sepCMA-ES solve around 30% of all problems, whereas LMCMA-ES is the best one, which solves 40%. However, QIU-NSA demonstrates the best performance on the separable functions and multi-modal problems with adequate global structure (see Figure 5). We can conclude that QIU-NSA efficiently scales NSGA-III down. Moreover, it is very efficient to solve the separable problems and shows a good scalability w.r.t. the dimensions of the search space. The main limitation of QIU-NSA is its non-invariance w.r.t. the function rotations.

3.2 Reproducing Physical Properties of MCMs

The objective of this experiment is to validate an efficiency of the proposed hybrid unified algorithm to solve a single-objective problem of the model of MCMs: i.e., to find a set of the parameters of the BEG-I model, which corresponds to the physical properties of the given MCM - *LaFeCoSi* (*LaFeSi(B)*).

3.2.1 Input Parameters, Reference Parameters and Values of Interest.

The input parameters and their boundary values are presented in Table 4 and the reference values of the output parameters are provided in Table 5. More details about the input parameters of the Hamiltonian of the BEG-I model and the optimization method for studying physical properties of MCMs can be found in [13].

Table 4: Input parameters and their boundary values (the Hamiltonian parameters for *LaFeSiCo* material)

Parameter	H_{field}	K	U_1	U_2	AA	A_{temp}
Value	0.1 - 2.5	0.1 - 2.5	0.1 - 2.5	$= U_1$	-	0.0-2.5

Table 5: Reference properties of *LaFeCoSi* material for objective functions provided by Crismat laboratory

Parameter [K]	T_{coolR}	T_{warmR}	$\Delta T_{cv_{coolR}}$	$\Delta T_{cv_{warmR}}$
$H_0 = 0[T]$	238.5	239.3	6.0	6.0
$H_1 = 2[T]$	245.5	246.0	12.0	12.0

Objective function is defined as follows:

$$F = F_{cool} + F_{warm} \quad (2)$$

$$F_{cool} = |(\Delta T_{cv_{coolR}}(H_0) - \Delta T_{cv_{cool}}(H_0))| + |(\Delta T_{cv_{coolR}}(H_1) - \Delta T_{cv_{cool}}(H_1))| \quad (3)$$

$$F_{warm} = |(\Delta T_{cv_{warmR}}(H_0) - \Delta T_{cv_{warm}}(H_0))| + |(\Delta T_{cv_{warmR}}(H_1) - \Delta T_{cv_{warm}}(H_1))| \quad (4)$$

where $\Delta T_{cv_{cool}}(H_0)$, $\Delta T_{cv_{warm}}(H_0)$, $\Delta T_{cv_{cool}}(H_1)$ and $\Delta T_{cv_{warm}}(H_1)$ is the the temperature interval width of heat capacity curve peak under different magnetic fields upon cooling and warming process.

3.2.2 Experimental Result. The values of the free parameters obtained by the optimization for *LaFeCoSi* are as follows: $H_{field} = 1 [T]$, $K = 0.80$, $U_1 = 0.85$, $A_{temp} = 1.00$. In the Figure 6, we report the temperature dependence of magnetic entropy change (ΔS), which are calculated by using the Maxwell's equation from the simulated (theoretical) data with obtained parameters and from the measured data of the Crismat Laboratory. The agreement between the theoretical and measured data is excellent: the Mean Absolute Percentage Error (MAPE) of ΔS is 0.1%.

3.3 Optimization of the AMR Design

Aiming at achieving the best technical-economical compromise for the industrial applications, we apply the proposed tool for developing an innovative architecture of the AMR, which will be compact, powerful and energy efficient for the Magnetic Refrigeration System (MRS) and the Thermo-Magnetic energy Generator (TMG) modes.

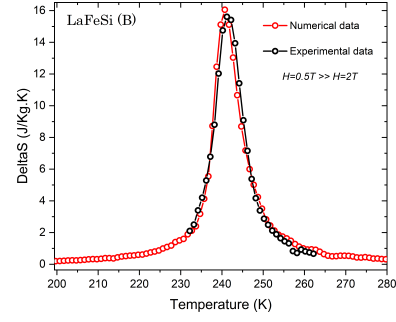


Figure 6: *LaFeCoSi*: The simulated and experimental temperature dependence of magnetic entropy change.

Table 6: The design and control parameters of the dual-mode operating AMR model

Parameter	Boundaries	Unit	Description
L	1-30	[cm]	AMR length along the direction of fluid motion
R_{vol}	0.05-1.5	[-]	Ratio of coolant volume transferred at each half AMR cycle on fluid volume
f	0.1-10	[Hz]	AMR operating frequency

3.3.1 Input Parameters, Reference Parameters and Values of Interest.

For this experiment, the most important input parameters of the AMR model, which have an impact in the both modes are selected and presented in Table 6 with their boundaries. R_{vol} and f are internal operating conditions that can control the thermodynamic cycles of the AMR, where L are the design parameters.

Since this research aims at finding the AMR configuration, which ensuring a good performance in two different application modes, 2 conflicting performance metrics for each mode are selected as the objective functions and presented in Table 7.

Table 7: Objective functions

Objective	Unit	Mode	Description
COP/COP_{Carnot}	[-]	MRS	Energy Efficiency
η/η_{Carnot}	[-]	TMG	Energy Efficiency
\dot{Q}_{cold}/V_{AMR}	$[W/cm^3]$	MRS	Thermal Power Density
\dot{W}_r/V_{AMR}	$[W/cm^3]$	TMG	Mechanical Power Density

The description of the objectives are presented below. The energy efficiency of the MRS is $\eta = COP/COP_{Carnot}$, where COP is the coefficient of performance and COP_{Carnot} is the Carnot coefficient of performance. The energy efficiency of the TMG is η/η_{Carnot} , where η_{Carnot} is the Carnot yield. The thermal power density of the MRS is \dot{Q}_{cold}/V_{AMR} , where V_{AMR} is the AMR volume ratio and \dot{Q}_{cold} is the refrigeration power. The mechanical power density of the TMG is \dot{W}_r/V_{AMR} , where \dot{W}_r is the recovery power.

The presented experiments are conducted with the other configuration parameters defined in Table 1.

3.3.2 Experimental Result. Figure 7 depicts the Pareto front of non-dominated solutions, showing in highlighted color values the MRS and TMG operating modes respectively. The Pareto front clearly reveals the conflict between the power densities and efficiency in both modes.

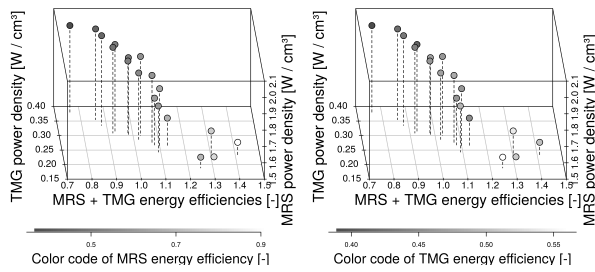


Figure 7: Obtained Pareto Fronts

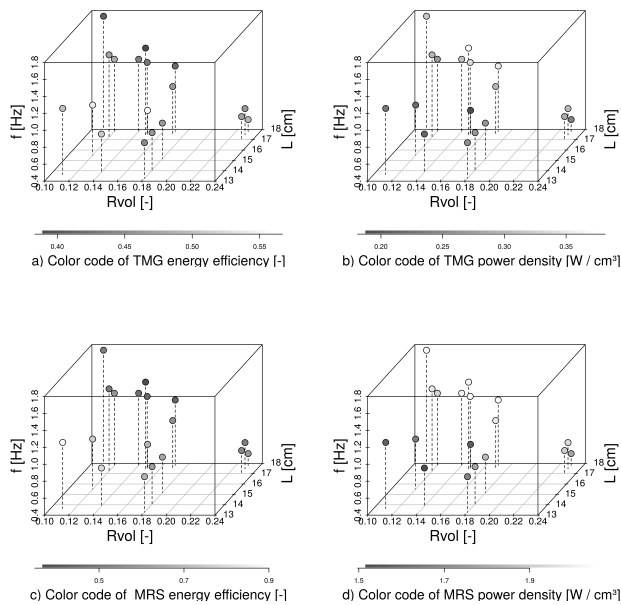


Figure 8: The distribution of Pareto optimal points solutions

A parametric study is conducted to investigate the effects of the variable parameters on the cycle performance through the power density and the efficiency. To make it clear, Figure 8 reports the distribution of Pareto-optimal solutions.

From Figure 8 a) it is seen that the maximum value of the energy efficiency of TMG is 0.56 [-], which is obtained for $L = 17.4$ [cm], whereas the value of $R_{vol} = 0.15$ [-] and $f = 0.69$ [Hz] is small. One can notice that the TMG efficiency range is quite small 0.39 – 0.56[-]. It can be explained by the fact that the pressure drop is

directly proportional to L and thus, a larger value of pressure drop greater penalizes the energy efficiency in the TMG mode. Figure 8 b) shows that the maximum value of the recoverable mechanical power density of the TMG is 0.37 [W/cm³], achieved with $f = 1.45$ [Hz], $R_{vol} = 0.15$ [-], and $L = 17.2$ [cm]. Thus, an increase of f leads to increase the mechanical power density and decrease the efficiency. The maximum value of the energy efficiency of the MRS is 0.56 [-] obtained with $L = 13.6$ [cm], $R_{vol} = 0.11$ [-] and $f = 1.18$ [Hz] (see Figure 8 c)). Figure 8 d) shows that the maximum value of the thermal power density of the MRS is 2,05 [-], which is achieved with the larger value of $L = 17.8$ [cm] and almost the same values of $f = 1.17$ [Hz] and $R_{vol} = 0.11$ [-] as for the the energy efficiency of the MRS.

We can conclude that for all criteria, R_{vol} has less impact than the others. According to Figure 7, there are several solutions, which ensure the balance between efficiency and power density for the both modes. The Pareto fronts has slightly discontinuous shape that be explained by a large number of the rejected solutions, because of their nonexistence in the both modes simultaneously. Thus, an evaluation of the energy conversion system is required by reconsidering some default parameters of the AMR model, e.g., the fluid channel thickness, which was set to optimally match a refrigeration system in this study. The further experiments are required for taking a larger number of parameters into account.

4 CONCLUSION

Optimization of the Active Magnetic Regenerator (AMR) design and reproducing physical properties of Magneto Caloric Materials (MCMs) are major challenges for the magnetic cooling industry. The tool we propose, thanks to the hybrid method and the EASEA platform, is a robust user-friendly instrument of reducing time for setting up different experiments. The functionality of proposed tool is centred from single- to many-objectives problems that makes it universal. Moreover, it can easily be adapted to different AMR models or MCMs models.

It is validated that the proposed tool allows users to reproduce the physical properties of MCMs and to obtain the detailed information about a relationship between the selected parameters and performance of the AMR in different application modes. In this work, we showed that a balance between the efficiency and the power density can be found for the two modes: the Magnetic Refrigeration System and the Thermo-Magnetic energy Generator.

Thanks to the proposed tool, it is now possible to accelerate the elaboration of a commercially available device, which will correspond to modern ecological and energy-saving requirements.

In addition, this work opens new research directions for an application of hybrid methods in order to scale up/down an optimization algorithm w.r.t. the number of objectives.

ACKNOWLEDGMENTS

This work is funded through ANR project CoolMagEvo (ANR-17-CE05-0036). The ANR is gratefully acknowledged for its financial support. As well as Ubilblue Company and Crismat Laboratory for their collaborations.

REFERENCES

- [1] M Balli, C Mahmed, O Sari, F Rahali, and JC Hadorn. 2011. Engineering Of The Magnetic Cooling Systems: A Promising Research Axis For Environment And Energy Saving. In *World Engineers' Convention*.
- [2] Pierre Collet, Evelyne Lutton, Marc Schoenauer, and Jean Louchet. 2000. Take it EASEA. In *International Conference on Parallel Problem Solving from Nature*. Springer, 891–901.
- [3] D Coulomb, JL Dupont, and A Pichard. 2015. The role of refrigeration in the global economy. *International Institute of Refrigeration: Paris, France* (2015).
- [4] Kalyanmoy Deb and Himanshu Jain. 2013. An evolutionary many-objective optimization algorithm using reference-point-based nondominated sorting approach, part I: solving problems with box constraints. *IEEE transactions on evolutionary computation* 18, 4 (2013), 577–601.
- [5] K Deb and S Tiwari. [n. d.]. Omni-optimizer: A generic evolutionary algorithm for global optimization. *European Journal of Operations Research (EJOR)* ([n. d.]).
- [6] Gao Fei, Li Zhuo-Qiu, and Tong Heng-Qing. 2008. Parameters estimation online for Lorenz system by a novel quantum-behaved particle swarm optimization. *Chinese Physics B* 17, 4 (2008), 1196.
- [7] Hadi Ganjehsarabi, Ibrahim Dincer, and Ali Gungor. 2016. Analysis and optimisation of a cascade active magnetic regenerative refrigeration system. *International Journal of Exergy* 19, 2 (2016), 143–160.
- [8] Nikolaus Hansen, Anne Auger, Steffen Finck, and Raymond Ros. 2012. Real-parameter black-box optimization benchmarking: Experimental setup. *Orsay, France: Université Paris Sud, Institut National de Recherche en Informatique et en Automatique (INRIA) Futurs, Équipe TAO, Tech. Rep* (2012).
- [9] Nikolaus Hansen, Fabian Gemperle, Anne Auger, and Petros Koumoutsakos. 2006. When do heavy-tail distributions help? In *Parallel Problem Solving from Nature-PPSN IX*. Springer, 62–71.
- [10] Amin Ibrahim, Miguel Vargas Martin, Shahryar Rahnamayan, and Kalyanmoy Deb. 2017. Fusion-based hybrid many-objective optimization algorithm. In *2017 IEEE Congress on Evolutionary Computation (CEC)*. IEEE, 2372–2381.
- [11] Andrej Kitanovski. 2020. Energy applications of magnetocaloric materials. *Advanced Energy Materials* 10, 10 (2020), 1903741.
- [12] Xiujuan Lei and Ali Fu. 2008. Two-dimensional maximum entropy image segmentation method based on quantum-behaved particle swarm optimization algorithm. In *2008 Fourth International Conference on Natural Computation*, Vol. 3. IEEE, 692–696.
- [13] Anna Ouskova Leonteva, Radia Hamane, Michel Risser, Anne Jeannin-Girardon, Pierre Parrend, and Pierre Collet. 2021. New Evolutionary Method for Studying Physical Properties of Magneto Caloric Materials. In *2021 IEEE Congress on Evolutionary Computation (CEC)*. IEEE, 973–980.
- [14] Shouyi Li, Ronggui Wang, Weiwei Hu, and Jianqing Sun. 2007. A new QPSO based BP neural network for face detection. In *Fuzzy information and engineering*. Springer, 355–363.
- [15] Sergiu Lionte, Michel Risser, and Christian Muller. 2021. A 15kW magnetocaloric proof-of-concept unit: Initial development and first experimental results. *International Journal of Refrigeration* 122 (2021), 256–265.
- [16] Ilya Loshchilov. 2014. A computationally efficient limited memory CMA-ES for large scale optimization. In *Proceedings of the 2014 Annual Conference on Genetic and Evolutionary Computation*. 397–404.
- [17] Obaid Ur Rehman, Jiaqiang Yang, Qiang Zhou, Shiyong Yang, and Shafiqullah Khan. 2017. A modified QPSO algorithm applied to engineering inverse problems in electromagnetics. *International Journal of Applied Electromagnetics and Mechanics* 54, 1 (2017), 107–121.
- [18] Obaid Ur Rehman, Shiyong Yang, and Shafi Ullah Khan. 2017. A modified quantum-based particle swarm optimization for engineering inverse problem. *COMPEL-The international journal for computation and mathematics in electrical and electronic engineering* (2017).
- [19] Michel Risser, Carmen Vasile, C Muller, and Arsène Noume. 2013. Improvement and application of a numerical model for optimizing the design of magnetic refrigerators. *international journal of refrigeration* 36, 3 (2013), 950–957.
- [20] Raymond Ros and Nikolaus Hansen. 2008. A simple modification in CMA-ES achieving linear time and space complexity. In *International Conference on Parallel Problem Solving from Nature*. Springer, 296–305.
- [21] Steven Roy, Sébastien Poncet, and Mikhail Sorin. 2017. Sensitivity analysis and multiobjective optimization of a parallel-plate active magnetic regenerator using a genetic algorithm. *international journal of refrigeration* 75 (2017), 276–285.
- [22] Haitham Seada and Kalyanmoy Deb. 2014. U-NSGA-III: A unified evolutionary algorithm for single, multiple, and many-objective optimization. *COIN report 2014022* (2014).
- [23] Jun Sun, Wei Fang, Xiaojun Wu, Vasile Palade, and Wenbo Xu. 2012. Quantum-behaved particle swarm optimization: analysis of individual particle behavior and parameter selection. *Evolutionary computation* 20, 3 (2012), 349–393.
- [24] Jun Sun, Jing Liu, and Wenbo Xu. 2007. Using quantum-behaved particle swarm optimization algorithm to solve non-linear programming problems. *International Journal of Computer Mathematics* 84, 2 (2007), 261–272.
- [25] R Teyber, PV Trevizoli, TV Christiaanse, P Govindappa, I Niknia, and A Rowe. 2018. Semi-analytic AMR element model. *Applied Thermal Engineering* 128 (2018), 1022–1029.
- [26] Radha Thangaraj, Millie Pant, Ajith Abraham, and Pascal Bouvry. 2011. Particle swarm optimization: hybridization perspectives and experimental illustrations. *Appl. Math. Comput.* 217, 12 (2011), 5208–5226.
- [27] Shanshan Tu, Obaid Ur Rehman, Sadaqat Ur Rehman, Shafi Ullah, Muhammad Waqas, and Ran Zhu. 2020. A novel quantum inspired particle swarm optimization algorithm for electromagnetic applications. *IEEE Access* 8 (2020), 21909–21916.
- [28] Xin Yao and Yong Liu. 1997. Fast evolution strategies. In *International Conference on Evolutionary Programming*. Springer, 149–161.
- [29] Zhang Zhisheng. 2010. Quantum-behaved particle swarm optimization algorithm for economic load dispatch of power system. *Expert Systems with Applications* 37, 2 (2010), 1800–1803.